

# Numerical Analysis of Crack Initiation Life on Tunnel Boring Machine Cutter Seat

LI Jie<sup>\*</sup>, ZHANG Xin, HUANG Yuanjun, SU Kang, HU Bo, GUO Jingbo

<sup>1</sup> School of mechanical engineering, Shijiazhuang Tiedao University, Shijiazhuang 050043, Hebei, China

Received 7 Apr 2022

Accepted 5 Sep 2022

## Abstract

Aiming at the fatigue failure of TBM cutter seat under alternating load, the theoretical calculation and numerical simulation analysis method of cutter seat crack initiation life are investigated. According to the rock breaking process of disc cutter, the stress spectrum of cutter seat is obtained. Through the finite element analysis of cutter seat, the dangerous point position of cutter seat is determined. Combined with Q345D material S-N curve and fatigue damage accumulation theory, the prediction model of cutter seat crack initiation life is established, and the prediction of cutter seat crack initiation life is realized. Finally, the crack initiation life of cutter seat is analyzed numerically. The results show that the dangerous part of the cutter seat is at the "L" shape corner, which is consistent with the actual situation. The crack initiation life of the cutter seat is  $9.46 \times 10^8$  times,  $3.00 \times 10^8$  times,  $2.13 \times 10^8$  times and  $1.25 \times 10^8$  times with the survival rate of 50%, 90%, 95% and 99%. The errors between the theoretical analysis and simulation analysis results are 4.6%, 4.3%, 2.0% and 8.4% respectively. The feasibility of the numerical analysis method and the correctness of the crack initiation life prediction mode of the cutter seat is verified.

© 2022 Jordan Journal of Mechanical and Industrial Engineering. All rights reserved

**Keywords:** Tunnel boring machine (TBM); Cutter seat; Crack initiation; Load Spectrum; Life prediction.

## 1. Introduction

Tunnel Boring Machine (TBM) is a highly mechanized and automated large-scale tunnelling equipment for excavation and lining, which has been widely used in tunnel construction projects in railway, municipal, highway, water conservancy and other fields[1-3]. The TBM breaks rock through cutters installed on the cutter head. The cutter shaft of cutter is fixed on the cutter seat through C-shaped blocks and bolts, and the box-type cutter seat is welded on the cutter head. The structure of cutter head and cutter seat is shown in Figure 1[4]. In the process of tunnelling, the cutter is driven by the thrust and torque provided by the cutter head to rotate around the cutter shaft while making the circular motion with the cutter head, and the cutter directly contacts with the rock. The cutter is acted by vertical force, tangential force and lateral force at the cutter ring when it is breaking the rock, as shown in Figure 2. Due to the uncertainty and step of geological rock in tunnelling, the load of cutter is complex in rock breaking, and the cutter seat bears the rock breaking load and strong impact from cutter, so the cutter seat is prone to crack, deformation and other failure problems under alternating load [5-6]. The fatigue crack propagation of the cutter seat structure will be caused once the cutter head cracks appear, which may delay the construction period and lead to major safety accidents.

Therefore, it is very important to study the fatigue failure of the cutter seat and predict the crack initiation life of the cutter seat in the design stage.

In recent years, many scholars have done a lot of research on fatigue crack failure of cutter head and cutter seat cracks of tunnel boring machine. Yang [7] based on the rock breaking mechanism of the central cutter seat, combined with the fatigue life curve of Q345D material and fatigue damage criterion, established a prediction model of crack initiation life of the central cutter seat, and predicted the fatigue life of the central cutter seat under full load. Liu [8] et al. established a calculation model of crack initiation life at dangerous points of TBM cutter head, and studied the influence of geological factors on crack initiation life at dangerous points and the influence of failure regional factors on residual crack initiation life at dangerous points. Ouyang[9] et al. used multi-body dynamics and finite element method, combined with statistical counting method to obtain the stress spectrum of cutter head, and established the crack initiation life model of cutter head according to the stress-life curve of materials. Huo [10] et al. proposed an improved quasi-static method to calculate the dynamic stress of the cutter head, and introduced the plastic constraint factor  $\alpha$  to change the yield stress value of the material, and proposed a small time scale fatigue crack growth model of the cutter head with plane stress-strain transition. Zhang [11] et al. modified the short-time scale crack propagation model considering the influence of residual stress, and predicted the crack propagation life of the weld of the cutter head in

\* Corresponding author e-mail: tbmlijie@126.com.

view of the fatigue crack problem at the weld of the split cutter head. Kheder, A. [12] et al. Studied the fatigue characteristics of as-cast acicular ductile iron (ASGI) produced by alloying and controlled cooling and as-rolled 42CrMo4 steel. Under the condition of alternating load, the fatigue failure of the structure mainly occurs, and the causes of fatigue failure of the cutter seat are summarized as the material of the cutter seat, working environment and load. Therefore, it is necessary to study the crack initiation life of the cutter seat based on the actual geological conditions of the project.

The tunnel boring machine in this paper is based on a tunnel construction bid section, whose diameter is 6470mm, and the cutter head contains 40 disc cutters. In the process of changing the cutters, 23 cracks were found in the cutter seat, which led to the shutdown to repair the cracks and reduced the construction efficiency greatly. The cracks in the cutter seat are shown in Figure 3. However, if the maintenance of the cutter seat is not carried out in time, the cutter head may crack and increase the construction

safety risk. Especially under complex geological conditions, the alternating load condition of the cutter seat is more severe, and the reliability decline of the cutter seat is more prominent [13].

To sum up, the stress spectrum of the cutter seat obtained through the simulation analysis of rock breaking of cutter, determines the dangerous position of the cutter seat on the basis of establishing the finite element model of the cutter seat, and the prediction model of the crack initiation life of the cutter seat was established based on the modified nominal stress legislation by combining the S-N curve of Q355 material and the fatigue damage accumulation theory, so as to realize the prediction of the crack life of the cutter seat. At the same time, nCode fatigue analysis software is used to verify the correctness of the prediction model of crack initiation life of cutter seat, which provides an effective method for studying crack initiation life of cutter seat.

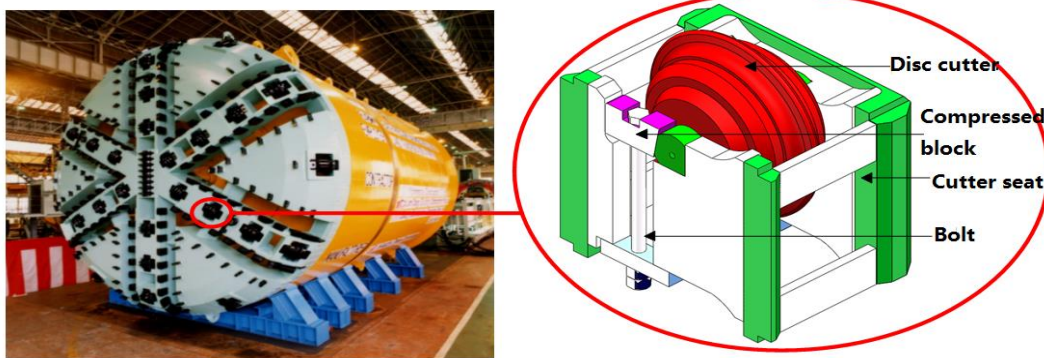
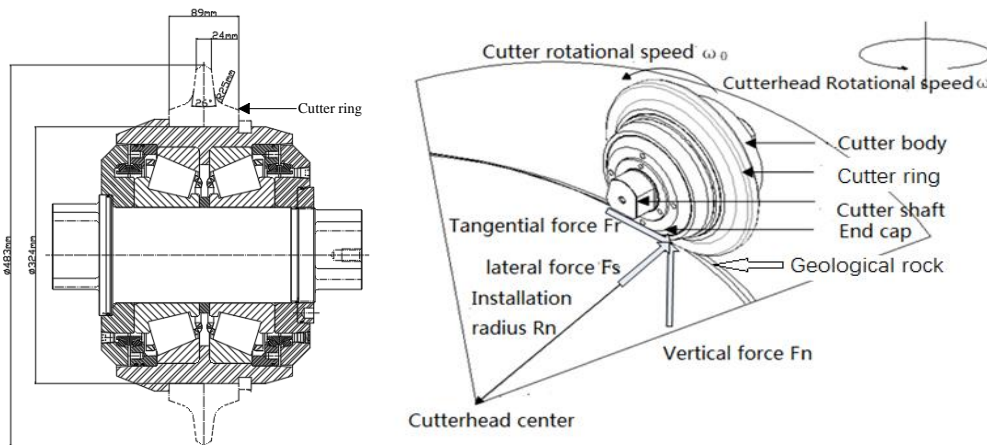


Figure 1. Cutter head and cutter seat



(a) Disc cutter structure and parameters (b) Rock breaking process and force of disc cutter

Figure 2. Disc cutter structure and rock breaking process

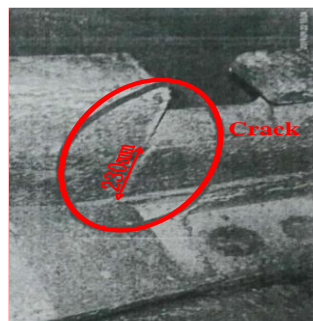


Figure 3. Crack diagram of cutter seat

## 2. Acquisition of stress spectrum of cutter seat of TBM

Aiming at the fatigue crack failure problem of TBM cutter seat under alternating load, the stress of cutter seat is obtained by simulation analysis of cutter rock breaking, and the load spectrum of cutter seat is obtained by statistical and counting methods. On the basis of determining the dangerous point position of cutter seat, the stress spectrum of dangerous point is obtained by loading the load spectrum of cutter seat, which provides theoretical basis for predicting the crack initiation life of cutter seat.

### 2.1. Acquisition of load spectrum of cutter seat

Many scholars have done a lot of research on the stress analysis of disc cutter. At present, the CSM disc cutter stress prediction model proposed by Colorado Institute of Mining and Technology is widely used, which comes from the summary of a large number of tunnel construction experiences and has strong practicability[14-15]. See the following formula for the force of disc cutter when it's breaking rock.

$$\begin{cases} F_t = \frac{P^0 \phi RT}{l + \psi} \\ \phi = \arccos\left(\frac{R-h}{R}\right) \\ P^0 = C_3 \sqrt{\frac{S}{\phi \sqrt{RT}}} \sigma_c^2 \sigma_t \end{cases} \quad (1)$$

In the formula (1),  $F_t$  is the resultant force (kN) of the disc cutter;  $R$  is the radius (mm) of the disc cutter;  $T$  is the blade width (mm) of disc cutter;  $\psi$  is the pressure distribution coefficient of the cutter tip, which decreases with the increase of the blade width, and the pressure distribution coefficient of the cutter tip is 0.2 ~-0.2;  $\phi$  is the contact angle (rad) between disc cutter blade and rock;  $h$  is the penetration of disc cutter (mm);  $P^0$  is the pressure of rock fracture zone, which is related to rock strength, disc cutter geometry, penetration and cutter spacing ( $P^0 = f(\sigma_t, \sigma_c, T, R, \phi, S)$ );  $C$  is a constant similar to rock contact angle  $\phi$ , and its value is 2.12;  $S$  is the cutter spacing (mm) of disc cutter;  $\sigma_c$  is the uniaxial compressive strength of rock;  $\sigma_t$  is the tensile strength of rock.

Because the simulation analysis method has better accuracy and economy, Abaqus software is used to simulate the rock breaking process of disc cutter. According to the actual disc cutter used in TBM, the 19-inch disc cutter model is adopted. Considering that only the cutter ring contacts with rock in the process of rock breaking, only the rock breaking simulation model of disc cutter ring is established. The rock breaking model of disc cutter is shown in Figure 4. The structural parameters of cutter ring are shown in Table 1.

**Table 1.** Structure parameters of cutter ring

Outer diameter of cutter ring	Inner diameter of cutter ring	Width of cutter ring	Blade width	Cutting edge angle	Fillet radius
483mm	324mm	89mm	24mm	26 °	25mm

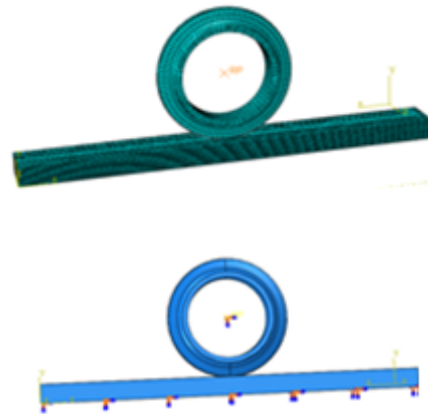


**Figure 4.** rock breaking model with disc cutter

The mesh type of disc cutter ring is hexahedral element, and the number of meshes is 2269. The mesh type of rock is hexahedral element, and the number of meshes is 43200. According to the field tunneling parameter data, the cutter head diameter is 6470mm, of the TBM is 7800mm, the cutter installation radius is 0.9 m, the cutter head rotation speed is 6.5 r/min, and the penetration is taken as the actual penetration average value of 5mm. The loads and constraints are set as follows: the translation speed of the cutter is 613mm/s, the rotation speed is 2.536 rad/s, and 5mm is pressed into the rock surface; the degrees of freedom at the bottom and both sides of the rock are all constrained.

The geological parameters are concluded that the geology traversed by the bid section of the project. It can be divided into four typical geology, and the compressive strength of rocks is 150 MPa, 120 MPa, 80 MPa and 40 MPa respectively. When the rock compressive strength is 150MPa, the physical parameters are: elastic modulus is 47.6 GPa, Poisson's ratio is 0.18, compressive strength is 150MPa, tensile strength is 4.2 MPa. Drucker-Prager strength criterion is selected as the failure criterion. The rock-breaking model of disc cutter is simulated by control variable method. After the rock-breaking simulation of disc cutter is completed, the stress of disc cutter is derived in the data post-processing module. Then, when the rock compressive strength is 120MPa, 80MPa and 40MPa, the stress of disc cutter breaking rock is obtained in turn, and then the load value of vertical force of disc cutter is derived and its average value is calculated. Then the vertical force is calculated according to CSM model, and the results of comparing them are shown in Table 2.

**Table 2.** Simulation and CSM model calculation results

Working condition	Rock compressive strength/MPa	Vertical Force Simulation Average/kN	CSM model calculation results/kN	Error value/%
Condition 1	150	231.129	247.456	6.5
Condition 2	120	191.029	203.251	6.0
Condition 3	80	157.832	162.741	3.0
Condition 4	40	98.412	102.52	4.0

It can be seen from Table 2 that with the increase of rock compressive strength, the vertical force on disc cutter also increases, and the average value of vertical force obtained by simulation is consistent with the calculation result of CSM model, and the relative error between them

is between 3% and 6.5%. The reason for the error is that the CSM model is fitted based on a large number of experimental data, and the geological parameters in the actual tunnelling are not a certain value, and the changes of the geological parameters will cause certain errors. In the Abaqus simulation model, the geological parameters are set to a certain value, and the mesh size and shape of the finite element model have a certain impact on the results.

Under the working condition 1, the cutter seat bears the maximum force, which is a dangerous working condition compared with others, and the characteristics of fatigue crack initiation life of the cutter seat are more obvious. Therefore, the rain flow counting method [16] is used to analyze the cutter seat load during rock breaking under the working condition 1, and the load amplitude is tested for normal distribution, and the function normplot is executed. If a straight line is obtained, it obeys normal distribution, and the test result is shown in Figure 5. Jarque-Bera test is used to test the goodness of fit of the amplitude of normal distribution, and the results show that the amplitude of the resultant force of working condition one accords with the normal distribution. Same as above, the load amplitude of working condition 2, working condition 3 and working condition 4 is also tested by normal distribution, and the results show that it also conforms to normal distribution.

Based on the normal distribution, the load data is expanded first and then synthesized to compile the 8-level load spectrum of the cutter seat [17], and the finally obtained 8-level load spectrum of the cutter seat is shown in Table 3.

2.2. Acquisition of stress spectrum of cutter seat

The cutter seat model is introduced into ANSYS Workbench software [18-19]. The cutter seat material is

Q355, the limit load is 320kN, the boundary conditions and the meshes are divided by tetrahedral and hexahedral elements. The number of meshes is 24771 and the number of nodes is 45007. Static analysis is carried out on the cutter seat, and its stress and displacement nephogram is shown in Figure 6.

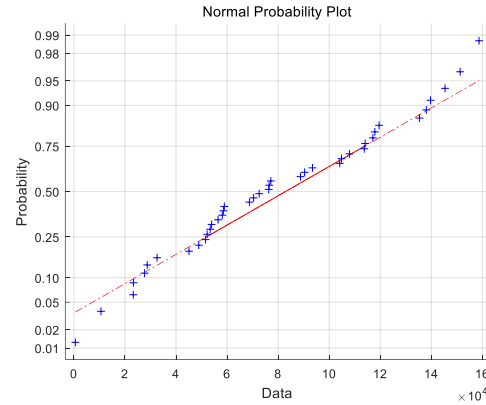


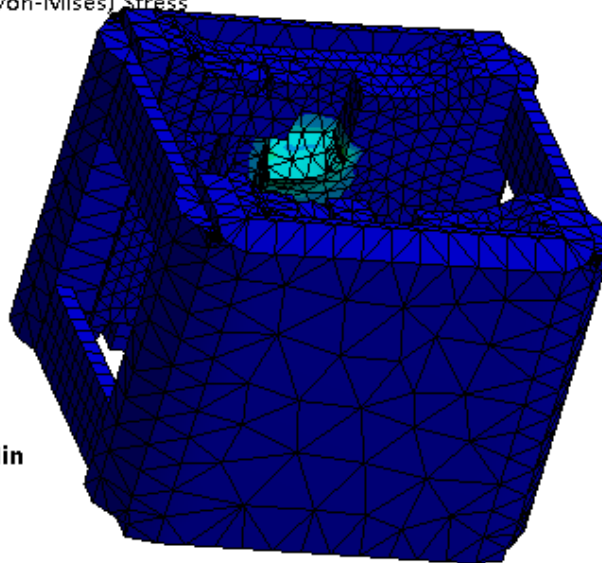
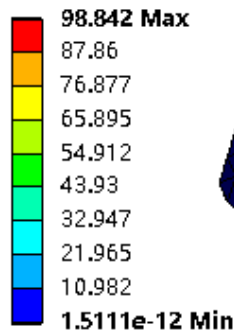
Figure 5. Normal distribution probability diagram of work condition 1

Table 3. The eight-level load spectrum

Load level	Load ratio coefficient	Load value/kN $X_i$	Number of load frequencies per stage	Cumulative frequency
1	1	300.31	1	1
2	0.95	290.758	1	2
3	0.85	271.656	7	9
4	0.725	247.776	45	54
5	0.575	219.121	363	417
6	0.425	190.466	2267	2684
7	0.275	161.812	10678	13362
8	0.125	133.157	36972	50334

A: Static Structural

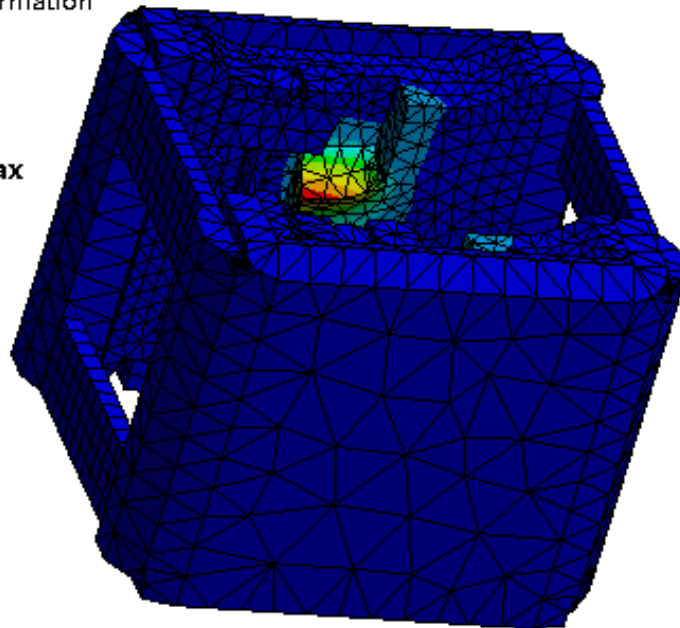
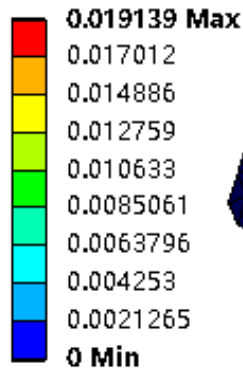
Figure  
 Type: Equivalent (von-Mises) Stress  
 Unit: MPa  
 Time: 1  
 2020/9/14 15:44



(a) The stress nephogram of cutter seat

**A: Static Structural**

Total Deformation  
 Type: Total Deformation  
 Unit: mm  
 Time: 1  
 2020/9/14 15:46



(b) The displacement nephogram of cutter seat

**Figure 6.** Stress and displacement nephogram

It can be seen from Figure 6, when the cutter seat bears the limit load, that the dangerous part is the corner of the "L" shape of the cutter seat, with the maximum stress of 98.842 MPa and the maximum displacement of 0.019 mm. The maximum stress of the cutter seat after loading does not exceed the strength of the cutter seat, which indicates that the structural part will not undergo plastic deformation. In this paper, it is assumed that there is no initial defect in the cutter seat structure, the crack initiation occurs at the stress concentration on the surface of the cutter seat, the plastic deformation does not occur when the cutter seat is loaded, and the fatigue type is high cycle fatigue, so the nominal stress method is used to calculate the crack initiation life of the cutter seat.

Load spectrum is the time history of load borne by parts. The load cycle type of cutter seat is asymmetric cycle. Considering the influence of average stress, Goodman formula is used to correct the stress amplitude [20], and the modified eight-level stress amplitude of cutter seat is shown in Table 4.

**Table 4.** Modified eight-level stress amplitude

Load level	1	2	3	4	5	6	7	8
Load value/kN	300.3	290.7	271.6	247.7	219.1	190.4	161.8	133.1
	1	58	56	76	21	66	12	57
Stress amplitude/MPa	92.68	89.73	83.83	76.47	67.93	59.04	50.16	41.28
	4	7	9		1	7	5	
Modified stress amplitude/MPa	99.87	94.54	90.34	82.40	73.20	63.62	54.05	44.48
	5	4	4	3	2	8	7	3

**3. Prediction of crack initiation life of cutter seat**

In order to predict the crack initiation life of the cutter seat, according to the stress spectrum of the dangerous

point of the cutter seat, combined with the S-N curve of the material Q345D and the fatigue damage theory, the traditional nominal stress method was modified considering the influence of stress concentration, geometric structure of the cutter seat and machining technology, and a prediction model of the crack initiation life of the cutter seat based on the modified nominal stress method was established to predict the cutter seat crack initiation life.

*3.1. Establishment of crack initiation life model of cutter seat*

Considering that it takes a lot of energy and financial resources to obtain the S-N curve of the cutter seat directly through experiments, this paper modifies the nominal stress method based on the S-N curve of materials. Also, considering the influence factors, such as stress concentration, size and surface machining, a prediction model of crack initiation life of the cutter seat is established based on the nominal stress method forming a prediction method of crack initiation life of the cutter seat, and realizing the crack initiation life prediction of cutter seat.

*3.1.1. Modification of nominal stress method*

The nominal stress method is often used to calculate the life of parts under high cycle fatigue. It is known that the fatigue life of the cutter seat is a high cycle fatigue generally, so the nominal stress method is selected to analyze the crack initiation life of the cutter seat [21]. The mathematical model of nominal stress method is

$$S^m N = C \tag{2}$$

Where,  $S$  is the stress value,  $N$  is the number of cycles, and  $m$  and  $C$  are the parameters related to the material of the structural part.

The nominal stress method is modified by using the correction coefficient, and the modified model is as follows

$$K_{\sigma} S^m N = \frac{C}{(K_{\sigma})^m} \quad (3)$$

The correction coefficient  $K_{\sigma}$  takes into account the comprehensive influence of stress concentration coefficient  $K_t$ , size coefficient  $\varepsilon$  and surface machining coefficient  $\beta$ , and the expression of the correction coefficient  $K_{\sigma}$  is as follows:

$$K_{\sigma} = \frac{1 + q(K_t - 1)\beta}{\varepsilon\beta} \quad (4)$$

Where:  $q$  is the sensitivity coefficient, which  $q$  is 0.6289 according to the situation of the cutter seat; the surface machining coefficient  $\beta$  is 0.75.

The stress concentration factor and size factor can be solved by finite element calculation method [22]. By obtaining the best integration path of the cutter seat dangerous part, the nominal stress can be solved according to the stress field function on the integration path as follows:

$$\sigma_n = \frac{\int_0^L \sigma(L) dL}{L} \quad (5)$$

Where:  $\sigma_n$  is nominal stress, MPa;  $L$  is the path length, mm.

The stress concentration factor of structural parts  $K_t$  is:

$$K_t = \frac{\sigma_{\max}}{\sigma_n} \quad (6)$$

Where:  $\sigma_{\max}$  is the maximum stress, MPa.

Dimension coefficients  $\varepsilon$  is:

$$\varepsilon = \frac{\sigma_f}{\sigma'_f} \quad (7)$$

Where:  $\sigma_f$  is the fatigue limit of large specimen, MPa;

$\sigma'_f$  is the fatigue limit of small specimens, MPa.

Combined with the stress field strength method [23-24], it can be seen that the relationship between structural parts and fatigue limits of materials is as follows:

$$\sigma_{0r} = \frac{\sigma_r}{K_t} [f(x_1, x_2)]^{-1} \quad (8)$$

Where:  $\sigma_r$  is the fatigue limit of the material, MPa;  $\sigma_{0r}$  is the fatigue limit of structural parts, MPa;  $f(x_1, x_2)$  is the stress field function near the local maximum stress,  $x_1$  and  $x_2$  are the coordinate parameter of the plane field.  $f(x_1, x_2)$  can be expressed by the distance  $L$  between the node and the maximum stress point under the integral path, that is,

$$f(x_1, x_2) = \omega_1 + \omega_2 L(i) + \omega_3 L^2(i) + \omega_4 L^3(i) \quad (9)$$

The above formula is solved simultaneously, and the calculation formula of size coefficient is:

$$\varepsilon = \frac{\int_0^L (\omega_1 + \omega_2 L + \omega_3 L^2 + \omega_4 L^3) dL}{\int_0^L (\delta_1 + \delta_2 L + \delta_3 L^2 + \delta_4 L^3) dL} \quad (10)$$

Where:  $\omega_i$  and  $\delta_i$  are the coefficients of the stress field function.

### 3.1.2. S-N curve of cutter seat material

According to reference [23], the fatigue parameters of Q345D under different survival rates can be found out. By fitting the fatigue parameter data, the mathematical expression of P-S-N curve of Q345D under different survival rates is as follows. The fatigue fitting curves of Q345D under different survival rates are shown in Figure 7.

The expression of survival rate is 50% expression:  $S = 1202 \times N^{-0.1276}$

The expression of survival rate is 90% expression:  $S = 1435 \times N^{-0.145}$

The expression of survival rate is 95% expression:  $S = 1524 \times N^{-0.1509}$

The expression of survival rate is 99% expression:  $S = 1726 \times N^{-0.1631}$

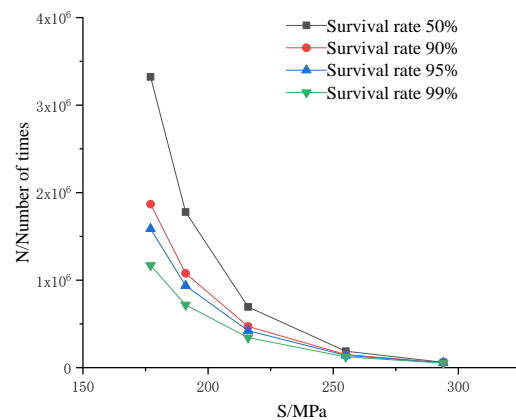


Figure 7. P-S-N Curve of Q345D

### 3.1.3. S-N curve of cutter seat

The S-N curve of the cutter seat is  $S^m N = \frac{C}{(K_{\sigma})^m}$ ,

where the correction coefficient is  $K_{\sigma}$ . Based on the finite element analysis results of the cutter seat, the best integration path is selected at the maximum stress point, as shown in Figure 8. The stress values corresponding to different path lengths on the integration path are shown in Table 5.

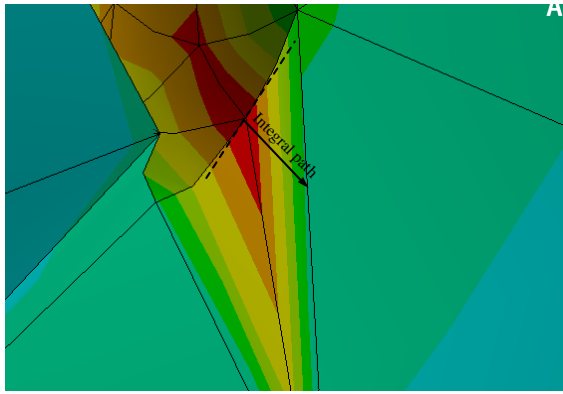


Figure 8. Cutter seat integrated path

Table 5. Integrated path stress values

L/mm	S/MPa
0	98.842
2.275	93.41
5.6875	87.588
...	...
40.95	68.103
50.05	43.55
54.6	20.717

The stress field function obtained by fitting the data in Table 5 is:

$$S = -0.002186x^3 + 0.1753x^2 - 4.522x + 103.333 \quad (11)$$

According to Equations (6), (10) and (11), the stress concentration factor and dimension factor of the cutter seat are calculated to be 1.43 and 0.9546 respectively.

The stress concentration factor  $K_t$ , dimension factor  $\epsilon$  and surface machining factor  $\beta$  are substituted into equation (4), and the result  $K_\sigma$  is 1.68.

After correction, the P-S-N curve of the cutter seat is shown in Figure 9, and the mathematical expression is:

Survival rate 50% expression:  $S^{7.837} N = 2.351 \times 10^{22}$

Survival rate 90% expression:  $S^{6.897} N = 1.651 \times 10^{20}$

Survival rate 95% expression:  $S^{6.627} N = 3.983 \times 10^{19}$

Survival rate 99% expression:  $S^{6.131} N = 2.917 \times 10^{18}$

The fatigue life curves of the cutter seat under different survival rates can be obtained from Figure 9. It can be seen from Figure 9 that when the survival rate increases, the fatigue strength of the cutter seat decreases and the fatigue life will be shortened. The fatigue life curve of cutter seat provides a theoretical basis for crack life prediction of cutter seat.

### 3.2. Prediction of cutter seat crack initiation life

According to Miner's fatigue damage accumulation theory [22], when the structural member  $r$  is under the action of different stresses  $S_i$ , the fatigue failure life corresponding to each stress level is  $N_i$ , and the damage

$$D = \sum_{i=1}^r \frac{n_i}{N_i}$$

level is  $n_i$ . At that time  $D = 1$ , the structural member is damaged.

The number of cycles that can bear the load spectrum when fatigue failure occurs at the dangerous part of the cutter seat is  $\delta$ , and its mathematical expression is:

$$\delta = \frac{1}{D} \quad (12)$$

The expression of fatigue life of cutter seat is:

$$N = \delta \sum_{i=1}^8 n_i \quad (13)$$

Therefore, the fatigue crack initiation life of the cutter seat under different survival rates can be obtained as shown in Figure 10.

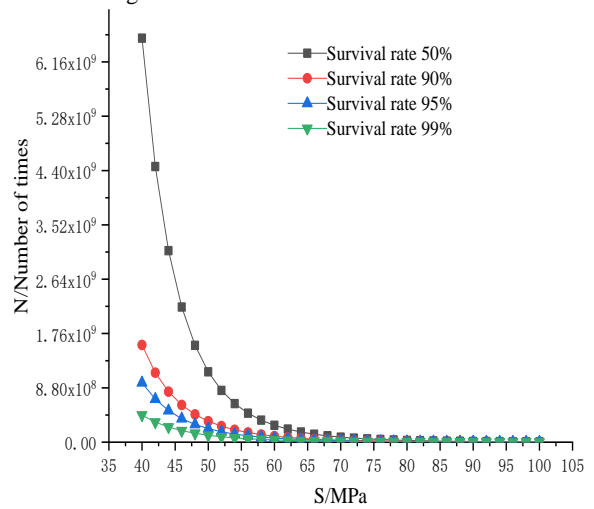


Figure 9. P-S-N curve of cutter seat

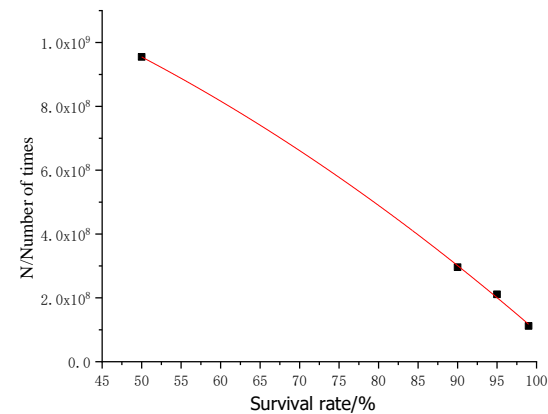


Figure 10. Fatigue crack initiation life of Cutter seat

Fitting from the data in the above figure, the fitting formula is as follows:

$$N = -8.3 \times 10^4 x^2 - 4.66 \times 10^6 x + 1.40 \times 10^9 \quad (14)$$

Where  $x$  is the survival rate. The crack initiation life of the cutter seat decreases with the increase of the survival rate, and the function relationship presents an inverse convex function relationship. When the survival rate increases from 50% to 90%, the crack initiation life decreases, and when the survival rate increases from 90% to 99%, the crack initiation life continues to decrease and the change rate increases.

#### 4. Simulation analysis of crack initiation life of cutter seat based on nCode

The finite element model of the cutter seat, S-N curve and load spectrum of the cutter seat are introduced into nCode software, and the fatigue analysis process is

established. When the survival rate is set to 50%, 90%, 95% and 99%, the crack initiation life of the cutter seat is solved respectively, and the distribution nephogram of the crack initiation life of the cutter seat is obtained as shown in Figure 11.

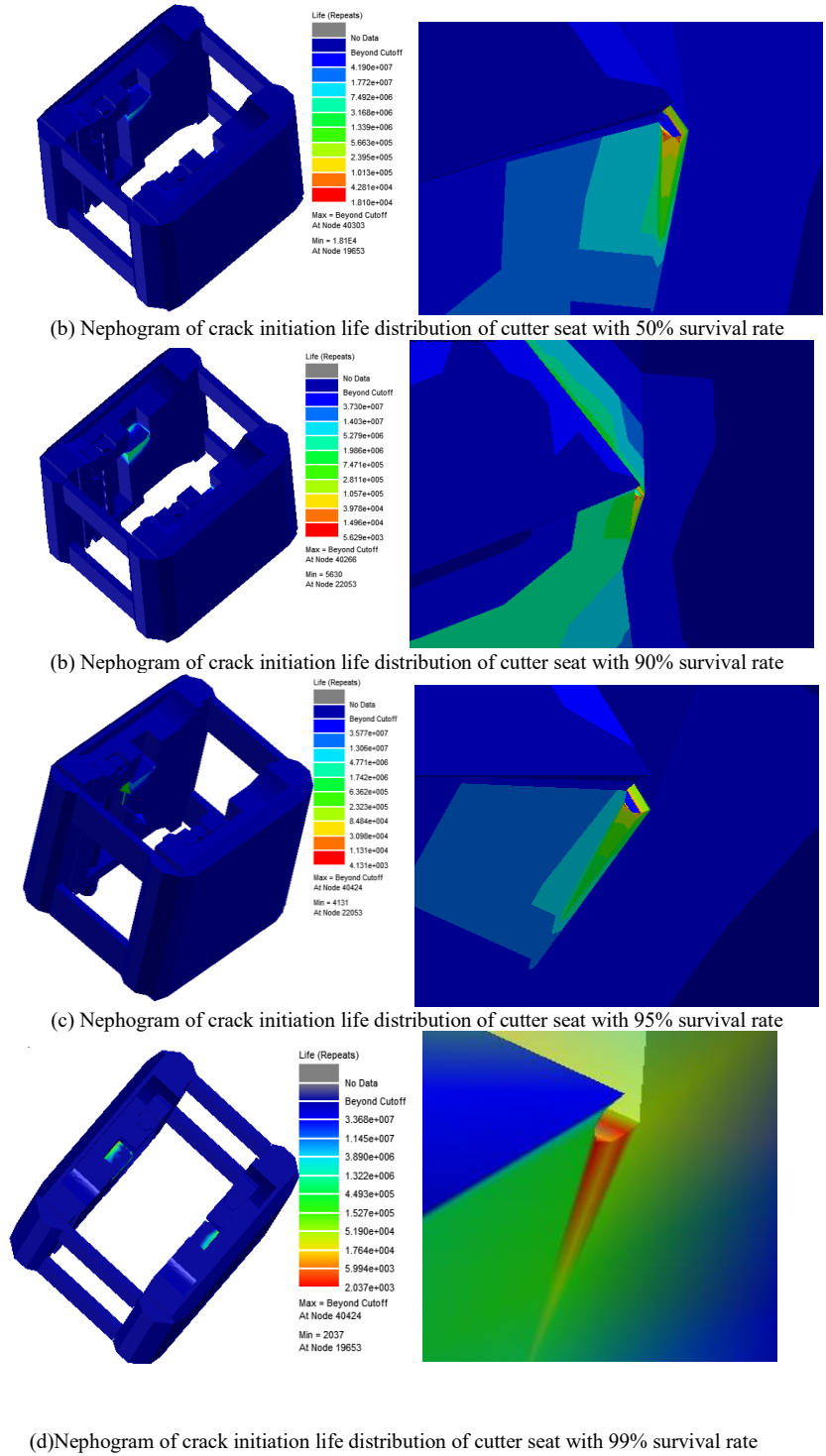
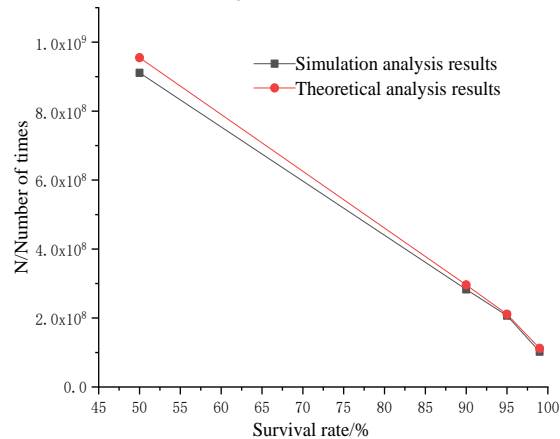


Figure 11. Fatigue analysis results of cutter seat under different survivor rates

As can be seen from Figure 11, the first crack initiation position is the corner of the "L" shape of the cutter seat. When the survival rate is 50%, 90%, 95% and 99%, the crack initiation life of the cutter seat simulated by nCode is  $9.11 \times 10^8$ ,  $2.83 \times 10^8$ ,  $2.07 \times 10^8$  and  $1.03 \times 10^8$  times respectively.

The fatigue crack initiation life of the cutter seat obtained by fatigue life simulation analysis of the cutter seat is compared with the fatigue crack initiation life of the cutter seat calculated based on the modified nominal stress method, as shown in Figure 12.



**Figure 12.** Comparison of fatigue life results of cutter seat under different survival rates

As can be seen from Figure 12, with the increase of survival rate, the crack initiation life of the cutter seat decreases. The simulation results have the same trend with the calculation results. The error between the simulation results and the theoretical analysis results is 4.6%, 4.3%, 2.0% and 8.4% when the survival rate is 50%, 90%, 95% and 99%, respectively. The error between the theoretical calculation results and the simulation results is small, which verifies the correctness of the prediction model of cutter seat crack initiation life. The causes of errors are mainly caused by the following points: Firstly, the correction coefficient mainly considers stress concentration coefficient, size coefficient and surface machining coefficient, but does not fully consider other influencing factors; Secondly, the meshing accuracy of the cutter seat has a certain influence on the fatigue crack initiation life of the cutter seat by using simulation method.

## 5. Conclusion

Aiming at the crack failure problem of TBM cutter seat under alternating load, the theoretical calculation and numerical simulation analysis of crack initiation life of TBM cutter seat are carried out in this paper, and the main conclusions are as follows:

1. The statics analysis of the cutter seat is carried out, and the crack initiation position is determined at the corner "L" shape of the cutter seat. The maximum stress under the ultimate load is 98.842 MPa, and the maximum deformation is 0.019 mm.
2. Considering the influence of stress concentration, geometrical dimension and surface machining, the prediction model of cutter seat crack initiation life based on modified nominal stress method is established, and

the crack initiation life of cutter seat with survival rate of 50%, 90%, 95% and 99% is calculated as  $9.46 \times 10^8$ ,  $3.00 \times 10^8$ ,  $2.13 \times 10^8$  and  $1.25 \times 10^8$  times respectively.

3. Based on the results of statics analysis, the numerical simulation of crack initiation life of cutter seat is analyzed using ANSYS nCode software. When the survival rate is 50%, 90%, 95% and 99% of the cutter seat, the crack initiation life of the cutter seat is  $9.11 \times 10^8$ ,  $2.83 \times 10^8$ ,  $2.07 \times 10^8$  and  $1.03 \times 10^8$  times. The error between the results and the theoretical analysis is 4.6%, 4.3%, 2.0% and 8.4%, respectively. The error is small, which verifies the correctness of the prediction model of the crack initiation life of the cutter seat.

## Conflicts of interest

There are no conflicts of interest.

## Acknowledgments

This work is financially supported by the Research & Development project of Hebei Province (22351901D), the Major National Research & Development project of china (2020YFB1709502), the Hebei Natural Science Foundation Project (E2019210275 and E2019210104) and the Science Research Project of the Education Department of Hebei Province (Grant No. ZD2021093)

## References

- [1] Zhang K . The Study on Feasibility and Welding Characteristics of GMAW Surfacing Remanufacturing of H13 Steel Cutter Ring of TBM Hob[J]. Coatings, 2021, 11.
- [2] Mifkovic M ,Swidinsky A , Mooney M . Imaging ahead of a tunnel boring machine with DC resistivity: A laboratory and numerical study[J]. Tunnelling and Underground Space Technology, 2021, 108:103703.
- [3] J Huo, Zhang Z ,Meng Z , et al. Dynamic Analysis and Experimental Study of a Tunnel Boring Machine Testbed under Multiple Conditions[J]. Engineering Failure Analysis, 2021, 127(5):105557.
- [4] ZHANG Wei, YUAN Chao-wei, CHENG Yong-feng, et al. Weld Performance Analysis and Structural Design of TBM Cutter head[J]. Modular Machine Tool & Automatic Manufacturing Technique, 2021(05): 153-156+160.
- [5] LI Hongliang. Troubleshooting for disc cutter cracking of model TB880E rock tunneler[J]. Construction Machinery, 2010, 41(03): 62-67+4. (in chinese)
- [6] Jingxiu Ling, Wei Sun, Junzhou Huo, Li Guo. Study of TBM cutter head fatigue crack propagation life based on multi-degree of freedom coupling system dynamics[J]. Computers & Industrial Engineering, 2015, 83: 1-14.
- [7] Yang Yun. Prediction of crack initiation life of shield machine center cutter seat[J]. Modern Manufacturing Engineering, 2020(10): 143-147. (in chinese)
- [8] Liu Jianqin, Ji Xuanbin, Guo Wei, et al. Study on geological matching and failure of TBM cutter head based on crack initiation [J]. Journal of Tianjin University (Natural Science and Engineering Technology Edition), 2017, 50 (11): 1148-1153. (in chinese)
- [9] Ouyang Xiangyu, Sun Wei, Huo Junzhou. Crack initiation life prediction of TBM cutter head under multi-point distributed load [J]. Mechanical Science and Technology for Aerospace Engineering, 2016, 35 (10): 1484-1488.
- [10] Huo J Z, Zhu D, Hou N, et al. Application of a small-timescale fatigue, crack-growth model to the plane

- stress/strain transition in predicting the lifetime of a tunnel-boring-machine cutter head[J]. *Engineering Failure Analysis*, 2016, 71: 11-30
- [11] Shuli Zhang, Jianfu Zhang, ZhongGuo, Peng Gao, Tianyu Du. Welding Residual Stress Characteristics of Boltwelding Joint in TBM Split Cutter head[C]//Proceedings of 2019 International Conference on Electronical, Mechanical and Materials Engineering(ICE2ME 2019). 2019:118-121.
- [12] Kheder, A., R., I., Jubeh, N., M., Tahah, E., M. Fatigue Properties under Constant Stress/Variable Stress Amplitude and Coaxing Effect of Acicular Ductile Iron and 42 CrMo4 Steel.[J]. *Jordan Journal of Mechanical and Industrial Engineering*, 2011, 5(4):301-306.
- [13] Cai Zheng. Study on safety risk management of subway tunnel shield construction[D]. China University of mining and technology, 2016. (in chinese)
- [14] Rostami J, Ozdemir L, Nilsen B. Comparison between CSM and NTH Hard Rock TBM Performance Prediction Models[C]//Proceedings of Annual Technical Meeting of the Institute of Shaft Drilling Technology. Las Vegas, 1996:1-10.
- [15] J Li, Nie YF, Fu K, et al. Experiment and analysis of the rock breaking characteristics of disc cutter ring with small edge angle in high abrasive grounds[J]. *Journal of the Brazilian Society of Mechanical Sciences & Engineering*, 2018, 40(10).
- [16] Ouyang Xiangyu. Life prediction of TBM cutter head crack initiation propagation under multi-point impact [D]. Dalian University of technology, 2015. (in chinese)
- [17] Bian Ye. Compilation of load spectrum of disc cutter of Full Face Rock Roadheader[D]. Northeastern University, 2009. (in chinese)
- [18] Emad A M, Ibrahim R. An Application of Finite Element Method and Design of Experiments in the Optimization of Sheet Metal Blanking Process[J]. *Jordan Journal of Mechanical and Industrial Engineering*, 2008, 2(1): 53-63.
- [19] Zhenqi Yu, Huifang Jia, Xingyuan Huang. Vibration Fatigue Analysis and Optimization Design of a Lighttruck Ur a Box Bracket[J]. *Jordan Journal of Mechanical and Industrial Engineering*, 2020, 14(1):167-173.
- [20] YANG Long, YANG Bing, YANG Guangwu, et al. Analysis on fatigue characteristics of spot welded joints of stainless steel car body[J]. *Transactions of the China Welding Institution*, 2020, 41(07):18-24+52+97-98. (in chinese)
- [21] CHEN Zhuo-yi, LI Chuan-xi, KE Lu, et al. Fatigue Crack Repair and Optimization of Cope Holes in Orthotropic Steel Decks[J]. *China Journal of Highway and Transport*, 2021, 34(07):301-312. (in chinese)
- [22] JIANG Yong. Three dimensional stress concentration and crack analysis of aviation connecting structure[D]. Nanjing University of Aeronautics and Astronautics, 2009. (in chinese)
- [23] Editorial board of mechanical engineering material performance data manual. *Mechanical engineering material performance data manual*[M]. Machinery Industry Press, 1995. (in chinese)
- [24] HUANG Jian, LI Chao-yang, CHEN Bing-kui. Mechanical behaviors of cross roller bearings with raceway roundness error[J]. *Journal of Central South University*, 2021, 28(07):2091-2104.